Journal of Solid Mechanics Vol. 1, No. 2 (2009) pp. 137-147

Geometrical Optimization of the Cast Iron Bullion Moulds Based on Fracture Mechanics

A. Niknejad[1,*], M. Karami Khorramabadi[2], M.J. Sheikhpoor[1], S.A. Samieh Zargar[1]

[1]*Faculty of Engineering, Payame Noor University (PNU), Yazd Branch, P.O. Box: 89175-646, Yazd, Iran*
[2]*Department of Mechanical Engineering, Islamic Azad University, Khorramabad Branch, Khorramabad, Iran*

Received 6 June 2009; accepted 30 July 2009

ABSTRACT
In this paper, the causes of the crack initiation in cast iron bullion moulds in Meybod Steel Corporation are investigated and then some new geometrical models are presented to replace the current moulds. Finally, among the new presented models and according to the life assessment, the best model is selected and suggested as the replaced one. For this purpose, the three recommended moulds were modeled and analyzed by ANSYS software. First, a thermal analysis and then a thermo-mechanical coupled field analysis were performed on each three model. The results of the analysis are used to determine the critical zone. The critical zone is selected on the symmetric axis of the inner surface of the mould. By comparing the principle stress contours and temperature distribution contours of three models, one of the suggested models was selected as optimized geometrical model. Then, the crack modeling and the life assessment on the optimized model were implemented and the total life of the model was calculated. Comparison of the life of the optimized and the initial models shows an increase in the life of the suggested model. The results are verified with the experiments.

Keywords: Optimization; Fatigue; Creep; Crack propagation; Cast iron

1 INTRODUCTION

FAILURE of the structures under the alternative loads often happens gradually because of material properties reduction of the structures. Today, finite element method is one of the common ways to investigate the failure causes of the parts. The finite element method is used in analysis, optimization and designing of the structures [1]. The finite element analysis provides variable contours of stress, strain and displacement and results the information about stress and strain under the cyclic loadings.

The initiation and growth characteristic of the corrosion pits were investigated during the corrosion fatigue process using a replica technique by Ishihara et al. [2]. Xu and Yuan [3] carried out a computational analysis of mixed-mode fatigue crack growth in quasi-brittle materials using extended finite element methods. Some aspects of the energy based on the approach to fatigue crack propagation was presented by Ranganathan et al. [4]. Wang et al. [5] proposed an extended McEvily model for fatigue crack growth analysis of metal structures. Borrego et al. [6] performed fatigue crack propagation tests under high-low and low-high block loading sequences in aluminum alloy specimens. Jones et al. [7] examined some of the data that were first used to relate crack growth (da/dN) to the stress intensity factor (K). Kagawa et al. [8] performed fatigue crack propagation tests using specimens with multiple parallel edge notches at regular intervals. In their study, fatigue pre-cracks of uniform length were successfully introduced by eccentric tension–compression loading. Fatigue crack propagation tests were carried out under four-points bending loading. Herrera and Zapatro [9] studied fatigue crack closure numerically with 2D finite element models as alternative to experimental methods. In a few cases, fatigue crack closure behavior was analyzed with tri-

* Corresponding author.
E-mail address: niknejad@pnu.ac.ir (A. Niknejad).

dimensional models. Cojocaru and Karlsson [10] conducted an object-oriented modeling frame for simulating crack propagation due to cyclic loadings. The approach utilized the commercial finite element (FE) software package ABAQUS and its associated Python based scripting interface. The crack propagation was simulated by a generalized node release technique. Liljedahl et al. [11] investigated the retardation of the fatigue crack growth. Uematsu et al. [12] studied the fatigue behavior of SiC-particulate-reinforced aluminum alloy composites with different particle sizes at elevated temperatures. Castillo et al. [13] derived the general form of a physically valid crack growth model based on functional equations.

Fan et al. [14] made an effort to predict the crack growth of the stainless steel 304L based on a newly developed fatigue approach. The approach consisted of two steps: 1. elastic–plastic finite element analysis of the component and, 2. the application of a multi-axial fatigue criterion for the crack initiation and growth predictions based on the outputted stress–strain response from the FE analysis. The iterative numerical procedure was used for estimating the 3D crack front loading enhancements due to the action of the "liquid entrapment mechanism" (LEM) by Bogdanski and Lewicki [15]. Giner et al. [16] carried out a two-dimensional implementation of the X-FEM within the finite element software ABAQUS by means of user subroutines, and investigated the crack propagation in fretting fatigue problems. Niknejad et al. [17] investigated the life assessment of the copper slag pot using the finite element method and coupled field analysis within software NISA.

Reviewing the published works revealed that many researchers have investigated the crack propagation and life assessment of different parts. In this article, some new geometrical models of the cast iron bullion moulds are introduced to replace the current model that is analyzed in Ref. [1]. Then, the best model that has the longest life is selected as the new optimized model.

2 WORKING CONDITIONS OF THE MOULDS

The moulds used in casting process and manufacturing of cast iron bullions are one of the parts that crack in the working situations and under thermo-mechanical loads. Niknejad et al. [1] investigated the behavior of cast iron bar moulds that are used in Meybod Steel Co. via finite element method and by software ANSYS. During the casting process, the molten cast iron is carried by the melt pot [17] and then poured inside the moulds that are installed on a chain conveyor. Because of contiguity between the inner surface of the mould and the molten cast iron, the temperature of the surface increases quickly and so the mould will be under the high thermal stresses. In addition, the mould is under the mechanical stresses because of its weight and the weight of molten materials inside it. Thus, the mould is under both of the creep and fatigue modes.

After passing a distance of nearly 13.5m, both of the mould and the molten material become cold using a flow of the cold water and the molten cast iron will turn into the solid phase during the cooling process. At the end of the manufacture line, the moulds rotate around the last axis of the chain conveyor and convert (Fig. 1), so the produced bullions discharge. The continuous charging and discharging of the moulds affect the moulds under the alternative and variable thermo-mechanical stresses. One of the problems during the casting process is the fatigue cracks initiation in the moulds due to the variable loadings. Hundred moulds are installed on the chain conveyor. Therefore usually during the casting process, some moulds crack and it is impossible to stop the manufacture line and substitute the cracked moulds due to continuous casting process. Thus, the investigation of the crack propagation and prediction of the moulds life before and after the cracking are so important. In Ref. [1], the life assessment of the moulds using in Meybod Steel Co. (MSC) is calculated, numerically. In this paper, three new geometrical models of the cast iron bullion moulds are introduced for replacing the current model that is analyzed in [1].

Fig. 1
Discharging of the cast iron bullions from the moulds due to weight.

3 METALLOGRAPHY

A standard cubic sample of the current moulds using in MSC with the edge length of 1cm is provided and the metallography test performed to determine the type of material and the material properties of the current moulds. Fig. 2 shows a picture of the sample metallography. A cast iron bullion mould has a nominal capacity of 35 Kg and is of GGG50 ductile cast iron.

The geometry of the current mould is symmetric around its central axis. Fig. 3 shows a mould before utilization and Fig. 4 shows it after splitting. In MSC, twelve melt pots produce and discharge in each 24 hours, normally. Therefore, every two hours, a melt pot is transferred to the casting workshop to discharge. The working cycle time of each mould is approximately six minutes. In lieu of discharging each melt pot, every mould will charge and discharge three times. So every mould is used 36 times a day. In Ref. [1], the life of the current mould which was calculated equals to 2625 cycles, numerically, so the total longevity of the current mould is equal to 72 days. This value had a good correlation with the actual life of the current moulds using in MSC. This longevity is not from an economical standpoint by considering the expenses of manufacturing and substitution of the moulds. Thus, in this article three new models are suggested in order to the improvement and replacement of the current moulds.

4 THREE NEW GEOMETRICAL MODELS

A mould repeatedly charges and after approximately six minutes discharges. Every working cycle of the mould is formed from each charging until the next charge. Now, some new geometrical models are suggested to replace the current moulds. The general dimensions and supporting conditions of three new models are assumed to be compatible to the current moulds.

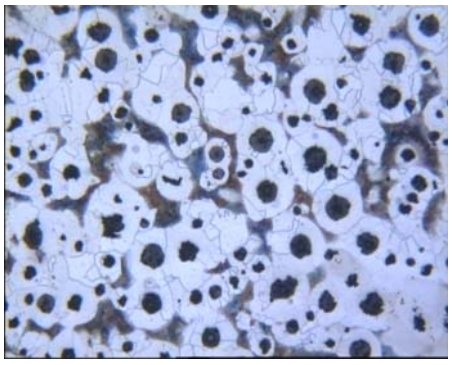

Fig. 2
A metallography image of the mould sample.

Fig. 3
A mould of cast iron bullion before utilization.

Fig. 4
A mould of cast iron bullion after splitting.

It makes installing the replacing models easy on the current chain conveyor. Fig. 5 shows three new geometrical suggested models to manufacture the new bullion moulds. The geometrical shape of three models and all mechanical and thermal loads are symmetric around the cross central axis. Notice that in the actual sample (Fig. 4), the crack initiates on the symmetric axis of the mould and in the middle of it, according to the Saint-Venant principle, the complete model of the mould is used in the numerical simulation.

5 THERMAL ANALYSIS

To the thermal analysis of the moulds and obtain the temperature distribution, the models No. 1, 2 and 3 are meshed with 60552, 73262 and 65020 elements, respectively. The elements type is 20-nodes Solid90 with thermal degree of freedom. The temperature of the inner surface of the model is assumed as same as the temperature of the molten cast iron. This temperature was measured to be $1200^{\circ}\mathrm{C}$. The outer surface and some parts of the inner surface of the model are exposed to the air with the temperature of $T_{\infty} = 35^{\circ}\mathrm{C}$ and the convection heat transfer coefficient of $h = 20\,\mathrm{w/m^2K}$. The molten cast iron is inside the mould for a short time and both of the mould and the melt become cold by the flow of the cold water just some minutes after pouring the melt into the mould, so the thermal analysis is solved transiently. The thermal material properties of the mould are given in Table 1. By applying the boundary conditions on the model, the temperature distribution contour was obtained as shown in Fig. 6. The maximum value of the temperature happens on the inner surface and is equal to the molten temperature.

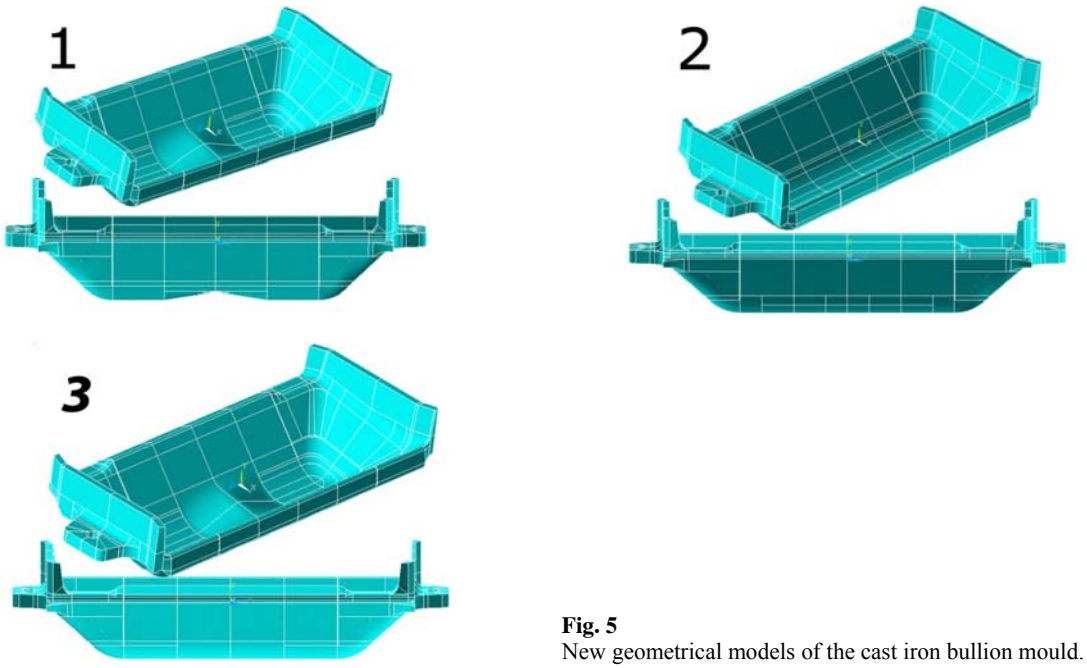

Fig. 5
New geometrical models of the cast iron bullion mould.

Table 1
Thermal properties of three new models

Melt temperature ($^{\circ}\mathrm{C}$)	Thermal conductivity ($\mathrm{w/m\cdot K}$)	Specific heat ($\mathrm{J/Kg\cdot K}$)	Thermal expansion coefficient ($1/^{\circ}\mathrm{C}$)	Air temperature ($^{\circ}\mathrm{C}$)	Convection coefficient ($\mathrm{w/m^2\cdot K}$)
1200	32.3	506	11.6×10^{-6}	35	20

From the inner surface of the mould to the outer surface, the temperature decreases and reaches to the air temperature. This coincides with the physical behavior of the mould. To the coupled analysis of the model in the next step, the temperature distribution of each model is saved as a separate file.

6 THERMO-MECHANICAL COUPLED FIELD ANALYSIS

For thermo-mechanical coupled field analysis, each three geometrical models were meshed using 20-Nodes Solid95 element with U_x, U_y and U_z degrees of freedom. The geometrical shape of this element is accurately similar to the previous thermal element. As the boundary conditions, the displacement of nodes inside the hole of the mould handle in all three directions was supposed to zero and the displacement of nodes inside the seat place of the mould handle on the support of the conveyor was supposed to be zero in the *Y* direction. The effect of the mould weight was applied on the model according to the data in Table 2 and by inserting the density of cast iron that is the material of the mould. Also, the molten cast iron weight was applied on the inner surfaces of the mould as different pressures. The results of the thermal distribution were applied on the model from the previous transient thermal analysis.

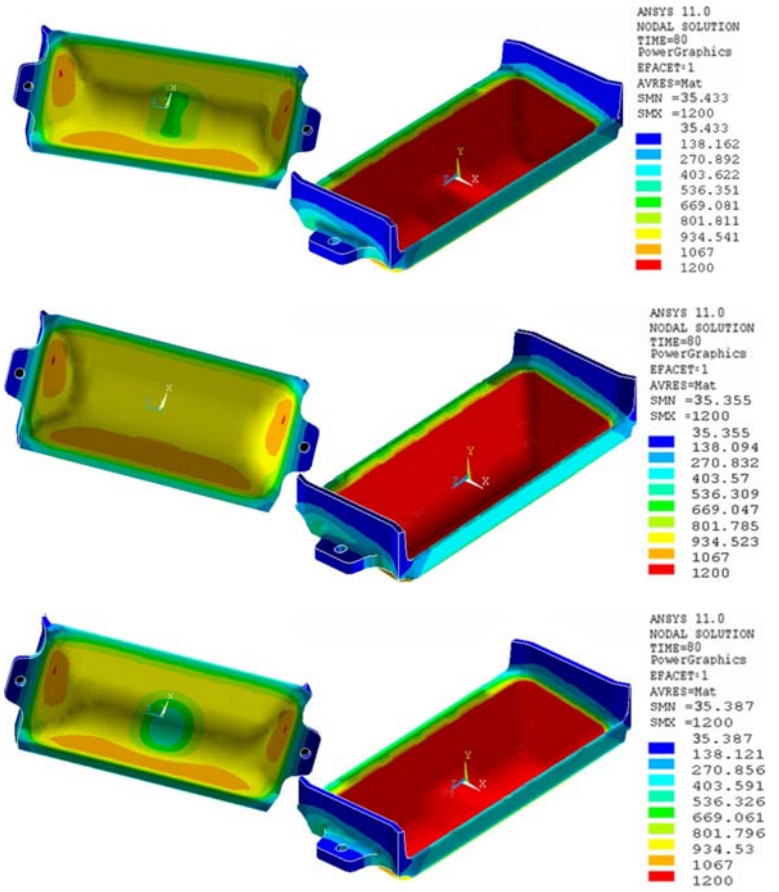

Fig. 6
The temperature distribution contour of three new models.

Table 2
Mechanical properties of the GGG50 cast iron

Poisson's ratio	Elasticity modulus (GPa)	Density (Kg/m^3)
0.25	172	7070

Fig. 7 shows the contours of the first principal stress as a result of coupled field analysis for every three models. The stress distribution contours in Fig. 7 show that the stress values around the hole of the mould handle and on the central axis of the mould are maximum value. In practice, crack initiates on the central part of the internal surface that shows a good correlation with the numerical results.

Notice that the center of the mould is under a high temperature and the crack initiates on this zone, the central area of the mould was selected as the critical zone and the crack was modeled in this area. Comparison of the obtained stress values in the critical zone from the numerical stress contours of three new models shows that the value of the normal stress of the model No. 3 is less than the other models and so, the model No. 3 is selected as optimized design. The semi-elliptical cracks were modeled in the optimized mould and developed during the six steps.

7 LIFE OF THE OPTIMIZED MODEL BEFORE CRACK INITIATION

The mould is under failure modes of creep and fatigue. Based on the Safe Life criteria, it is necessary to calculate the life of the mould due to failure modes, separately and then calculate the total life. To calculate the fatigue life, the General Slope method is used as following [17]:

$$\varepsilon_a = \frac{\sigma_f}{E}(2N_f)^b + \varepsilon_f (2N_f)^c \tag{1}$$

which is the Manson-Coffin relationship between fatigue life and total strain amplitude. In the above relation, σ_f is the fatigue strength coefficient, b is the fatigue strength exponent, ε_f is the fatigue ductility coefficient, and c is the fatigue ductility exponent. They are material properties. E, ε_a, and N_f are Elasticity modulus, strain amplitude and the number of cycles.

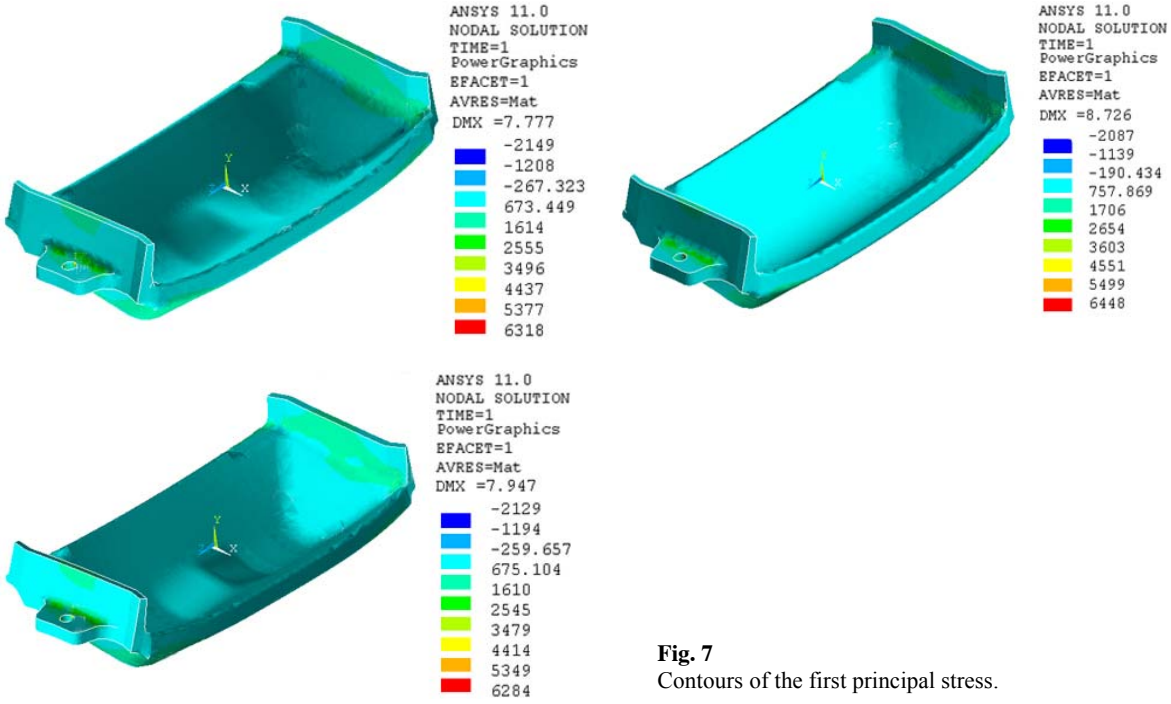

Fig. 7
Contours of the first principal stress.

Table 3
Coefficients of Eq. (1)

Fatigue ductility coefficient	Fatigue strength coefficient (MPa)	Fatigue strength exponent	Fatigue ductility exponent
0.45	1825	-0.75	-0.08

The coefficients of Eq. (1) for the material of the mould are given in Table 3. The amplitude of the strain obtained from the strain contour of the model No. 3 as a result of numerical analysis is equal to $\varepsilon_a = 2.64 \times 10^{-5}$. By substituting the value of the strain amplitude and the coefficients in Table 3 in Eq. (1), the fatigue life of the mould before the crack initiation obtains as:

$$N_f = 285 \text{ cycles} \tag{2}$$

The relationship between the strain rate, $\dot{\varepsilon}$, and the temperature of the part, *T*, are according to the following equation as Arenius equation [17]:

$$\dot{\varepsilon} = A \cdot e^{-\frac{Q}{RT}} \tag{3}$$

where *Q*, *R*, and *A* are the activation energy, the general constant and a stress-dependent coefficient, respectively. The creep life of the mould before the crack initiation is calculated using Larson-Miller parameter. The Larson-Miller equation is as follows [17]:

$$P_{LM} = T(C + \log t_r) \tag{4}$$

In the above equation, *T* is working temperature of the mould in Kelvin, t_r is the creep life of the mould, P_{LM} is the Larson-Miller parameter, and *C* is a constant which is defined as below [17]:

$$C = -\log(\theta_r) \tag{5}$$

where θ_r is a time-dependent parameter of the temperature. According to the stress contour in Fig. 7, the value of the applied stress on the mould in critical point was obtained equal to 134 MPa. Considering the critical stress value, the obtained value of the Larson-Miller parameter is equal to 30.3. By substituting this value into the Eq. (4), the obtained creep life of the mould is equal to 199524 minutes. A working cycle of the mould is about six minutes, thus, the number of the mould working cycles due to creep, N_C, is calculated as:

$$N_C = \frac{199524}{6} = 33254 \text{ cycles} \tag{6}$$

Using the linear damage criteria, the total life of the mould before the crack initiation is calculated as follows [1]:

$$\frac{1}{N} = \frac{1}{N_C} + \frac{1}{N_f} \tag{7}$$

Substituting the fatigue and the creep life of the mould from the Eq. (2) and (6), respectively, into the Eq. (7), the total life of the mould before crack initiation according to the Safe Life criteria is obtained as follows:

$$N = 282 \text{ cycles} \tag{8}$$

8 LIFE OF THE OPTIMIZED MODEL AFTER CRACK INITIATION

To investigate the fatigue crack growth, two parameters of the stress intensity factor, K and the creep integral, C^* are used. The applicability of K is limited to situations where the size of the crack tip creep zone is small relative to the crack length and other geometric parameters of the component. This is the so-called Small Scale condition (SSC), as opposed to the Steady State condition (SS) in which the crack propagation is accompanied by extensive creep deformation ahead of the crack tip. In the latter condition, the path-independent integral C^* is usually used. The transition time, t_1, for SSC condition to turn to SS condition can be estimated by [17]:

$$t_1 = \frac{1+2\beta_n}{1+n} \cdot \frac{K^2(t_1)\cdot(1-\nu^2)}{C^*(t_1)\cdot E} \tag{9}$$

in which β is dependent on the waveform of loading and is defined by [17]:

$$K(t) = K_1 t^{\beta} \tag{10}$$

where $K(t)$ is the applied stress intensity parameter as a function of time, and K_1 is a constant, v is the Poisson's ratio, n is the Norton Law exponent, and C^* is the creep integral. If the cycle time t_c is less than t_1, then, K is the correct crack tip parameter for correlating creep crack growth.

Notice that each working cycle of the mould is assumed six minutes, so the SSC is considered and K is used as the parameter controlling the crack growth. In this research, the point matching method is used to calculate the stress intensity factor. In this method, a relationship is established between the displacement of the nodal points and the parameters of the crack tip. Following a liner elastic analysis, the stress intensity factor can be determined by equating the numerically obtained displacements with their analytical expression in terms of the stress intensity factor. The mode I displacement equation is [1]:

$$u_i = \frac{K_I}{2G}\sqrt{\frac{2}{2\pi}} f_i(\theta,\nu) \tag{11}$$

where G and u_i are the energy release rate and the nodal point displacement, respectively. By replacing the displacement of the nodal points, u_i^* at some point (r,θ) close to the crack tip, quantity K_I^* is obtained as below [1]:

$$K_I^* = \sqrt{\frac{2\pi}{r}}\frac{2G}{f_i(\theta,\nu)}u_i^* \tag{12}$$

For the plain strain conditions of loading mode I and by substituting the $\theta = \pi$, K_I^* is obtained as the following [1]:

$$K_I^* = \frac{Gu_2^*}{2(1-\nu)}\lim_{r\to 0}\left(\sqrt{\frac{2\pi}{r}}\right) \tag{13}$$

First, a crack should be modeled in the optimized model of the mould to start the analysis of the crack propagation and the life-assessment. The critical zone is shown in Fig. 8 by a circle. The 3D semi-empirical crack was modeled in the critical zone and the singular elements are used in the crack tip zone. In order to determine an expression for parameters controlling the crack growth in terms of crack length, an incremental crack advance scheme was used. The crack was developed during six steps and with the crack length of 5-18mm. After each increment, the stress intensity factor, K_I was calculated using the Energy Domain Integral method. The stress intensity factor of each step is given in Table 4.

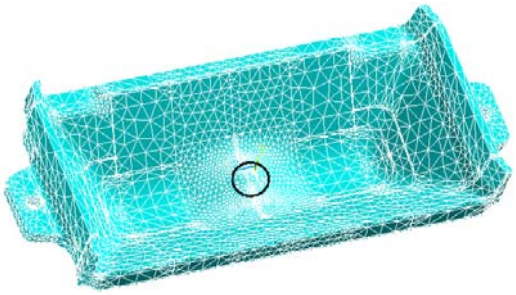

Fig. 8
The zone of the crack modeling in the optimized meshed model.

Table 4
The values of the stress intensity factor and the length of the semi-elliptical crack

Step	K_I (MPa$\sqrt{\text{m}}$)	a (m)
1	10.6629	0.005
2	14.0695	0.008
3	16.3760	0.010
4	17.6868	0.011
5	18.5959	0.014
6	20.1824	0.018

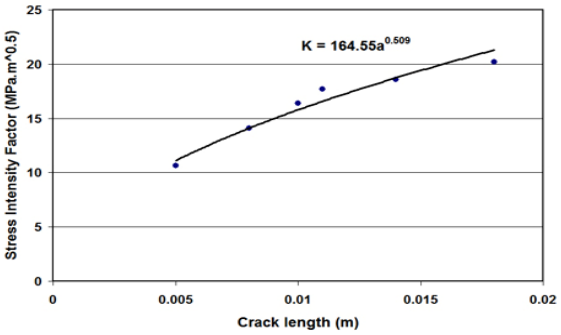

Fig. 9
Chart of the stress intensity factor versus the length of the semi-elliptical crack.

The diagram of the stress intensity factor versus the crack length is sketched in Fig. 9. The stress intensity factor, K_I varies versus the crack length a, by the below equation:

$$K_I = 164.5a^{0.509} \tag{14}$$

There is a creep crack development and a fatigue crack development in lieu of each working cycle. Thus, the total crack growth per working cycle, d*a*/d*N*, is expressed as [1]:

$$\frac{da}{dN} = C(\Delta K)^n + A\left[C(t)_{avg}\right]^m t_h \tag{15}$$

where *C*, *A*, *n*, and *m* are the material properties obtained from experiment and t_h is the cycle time of the mould. The first term of the above equation is the Paris equation that is calculated by the crack development in lieu of each cycle due to fatigue. The second term of the equation is computed the crack growth per cycle due to creep. Also, *C*(*t*) is the parameter controlling of the crack growth due to the creep and by its average value in each cycle is obtained as the following [1]:

$$C(t) = \frac{(1-\nu^2)K_I^2}{(1+n')Et} \tag{16}$$

where n' is a constant value that is equal to six. According to the working conditions and the material properties, the fatigue crack growth rate and the creep parameter is calculated as:

$$\left.\frac{\mathrm{d}a}{\mathrm{d}N}\right|_{Fatigue} = 12.1\times10^{-12}\Delta K^{2.715},\ \ C(t) = 0.02108a^{1.018} \tag{17}$$

Finally, by substituting the Eq. (17) in Eq. (15) and integration of the pertinent expression over the desired range of crack growth (0.2-60mm), the number of working cycles of the optimized model after the crack initiation is calculated to be 17940 cycles.

9 TOTAL LIFE

In order to calculate the total life of the optimized geometrical model, the sum of the mould lifes before and after the crack initiation is calculated as:

$$N_{tot.} = 17940 + 282 = 18222 \text{ cycles} \tag{18}$$

10 CONCLUSIONS

In this work and as the continuance of the previous research in Ref. [1], three new models is suggested for replacement of the current cast iron bar mould. These new geometrical models are designed and could be used without any change in the supports of the conveyor.

First, a thermal analysis and then a thermo-mechanical coupled field analysis are constructed on the three presented models. The temperature value of the numerical contours was compared with the measured values of the real moulds that is used in MSC by the laser thermometer which showed a good correlation. Further, the results of the thermo-mechanical coupled field analysis show that the maximum stress happens in the inner surface of the mould on the central area and the symmetric axis. In the model of the current moulds using in Meybod Steel Corporation, crack initiates exactly in this area, too. This comparison shows the correlation of the coupled field analysis results and the experimental results. The crack initiates from the inner surface of the mould and the temperature of this area is maximum. Thus, it is resulted that applying the high thermal stresses on the mould and the creep failure mode are the main causes of the crack creation. Further, the crack initiation begins from the central area of the inner surface of the mould and according to the supports conditions of the mold, here, the bending moment is the maximum. The weight force of the mould is constant but the weight of the molten materials inside the mould changes alternatively because of repeatedly charging and discharging. Therefore, applied mechanical stresses due to the weight and the fatigue failure mode are other causes of the crack creation. According to the results of the coupled field analysis, the central area of the inner surface of the mould is selected as the critical zone. By comparing the obtained stress values from the numerical stress contours of three new models in the critical zone, the model number 3 was selected as optimized design.

Then, life-assessment of the presented optimized model was carried out. For this purpose, the 3D semi-empirical crack was modeled in the critical zone and the singular elements are used in the crack tip zone. In order to determine an expression for parameters controlling the crack growth in terms of crack length, an incremental crack advance scheme was used. The crack was developed during six steps, with the length of 5-18mm. After each increment, the stress intensity factor K_I was calculated using the Energy Domain Integral method.

Finally, the number of working cycles was calculated by integration of the pertinent expression over the desired range of crack growth (0.2-60mm). The number of working cycles of the optimized model before and after the crack initiation was calculated as 282 and 17940 cycles, respectively. Thus, the obtained total life of the mould was equal to 18222 cycles. In Ref. [1], the number of the working cycles of the current mould using in Meybod Steel Corporation has been calculated to be 2625 cycles. Comparison of two lives shows an increase in the life of the new

presented mould with respect of the current mould about sixfold. The numerical results were verified with the experimental results that showed a good correlation.

REFERENCES

[1] Niknejad A., Samieh Zargar S.A., Sheikhpour M.J., 2009, Investigation of the life assessment and the crack propagation in the molds of cast iron bar, in: *Proceeding of the 17th International Conference on Mechanical Engineering,* Tehran, Iran (in Persian).

[2] Ishihara S., Nan Z.Y., McEvily A.J., Goshima T., Sunada S., 2008, On the initiation and growth behavior of corrosion pits during corrosion fatigue process of industrial pure aluminum, *International Journal of Fatigue* **30**: 1659-1668.

[3] Xu Y., Yuan H., 2008, Computational analysis of mixed-mode fatigue crack growth in quasi-brittle materials using extended finite element methods, *Engineering Fracture Mechanics* **30**: 1780-1786.

[4] Ranganathan N., Chalon F., Meo S., 2008, Some aspects of the energy based approach to fatigue crack propagation, *International Journal of Fatigue* **30**: 1921-1929.

[5] Wang Y., Cui W., Wu X., Wang F., Huang X., 2008, The extended McEvily model for fatigue crack growth analysis of metal structures, *International Journal of Fatigue* **30**: 1851-1860.

[6] Borrego L.P., Ferreira J.M., Costa J.M., 2008, Partial crack closure under block loading, *International Journal of Fatigue* **30**: 1787-1796.

[7] Jones R., Molent L., Pitt S., 2008, Similitude and the Paris crack growth law, *International Journal of Fatigue* **30**: 1873-1880.

[8] Kagawa H., Morita A., Matsuda T., Kubo S., 2008, Fatigue crack propagation behavior in four-points bending specimens with multiple parallel edge notches at regular intervals, *Engineering Fracture Mechanics* **75**: 4594-4609.

[9] Herrera A.G., Zapatero J., 2008, Tri-dimensional numerical modeling of plasticity induced fatigue crack closure, *Engineering Fracture Mechanics* **75**: 4513-4528.

[10] Cojocaru D., Karlsson A.M., 2008, An object-oriented approach for modeling and simulation of crack growth in cyclically loaded structures, *Advances in Engineering Software* **39**: 995-1009.

[11] Liljedahl C.D.M., Fitzpatrick M.E., Edwards L., 2008, Residual stresses in structures reinforced with adhesively bonded straps designed to retard fatigue crack growth, *Composite Structures* **86**: 344-355.

[12] Uematsu Y., Tokaji K., Kawamura M., 2008, Fatigue behavior of Sic-particulate-reinforced aluminum alloy composites with different particle sizes at elevated temperatures, *Composites Science and Technology* **68**: 2785-2791.

[13] Castillo E., Canteli A.F., Pinto H., Ruiz-Ripoll M.L., 2008, A statistical model for crack growth based on tension and compression Wohler fields, *Engineering Fracture Mechanics* **75**: 4439-4449.

[14] Fan F., Kalnaus S., Jiang Y., 2008, Modeling of fatigue crack growth of stainless steel 304L, *Mechanics of Materials* **40**: 961-973.

[15] Bogdanski S., Lewicki P., 2008, 3D model of liquid entrapment mechanism for rolling contact fatigue cracks in rails, *Wear* **265**: 1356-1362.

[16] Giner E., Sukumar N., Denia F.D., Fuenmayor F.J., 2008, Extended finite element method for fretting fatigue crack propagation. *International Journal of Solids and Structures* **45**: 5675-5687.

[17] Mirzaei M., Niknejad A., 2004, Investigation of the crack growth and life assessment of the copper slag pot, in: *Proceeding of the 12th International Conference on Mechanical Engineering,* Tehran, Iran (in Persian).